JOURNAL OF AGRICULTURAL AND FOOD CHEMISTRY

ARTICLE

pubs.acs.org/JAFC

Chain Length Effects in Isoflavonoid Daidzein Alkoxy Derivatives as Antioxidants: A Quantum Mechanical Approach

Cun-Bin An,[†] Dan Li,[†] Ran Liang,[†] Ya-Zhong Bu,[†] Sha Wang,[†] Er-Hai Zhang,[†] Peng Wang,[*,†] Xi-Cheng Ai,[†] Jian-Ping Zhang,[†] and Leif H. Skibsted[*,‡]

[†]Department of Chemistry, Renmin University of China, Beijing 100872, People's Republic of China

[‡]Food Chemistry, Department of Food Science, Faculty of Life Sciences, University of Copenhagen, Rolighedsvej 30, DK-1058 Frederiksberg C, Denmark

ABSTRACT: Daidzein, an isoflavonoid with known prooxidative effects in heterogeneous lipid/water systems, changes to an antioxidant for 7-*n*-alkoxy derivatives of daidzein. For an alkyl length increasing from 4 to 8, 12, and 16 carbons, the oxidation potential decreases gradually from 1.09 V (vs NHE) for daidzein (D) to 0.94 V for D16 in tetrahydrofuran as determined by cyclic voltammetry at 25 °C. The prooxidative effects transform into antioxidative effects from D8 with a maximal effect for D12 for aqueous phase initiation of lipid oxidation in liposomes despite a gradual decrease in Trolox equivalent antioxidant capacity (TEAC) with increasing alkyl chain length. Quantum mechanical calculations using density functional theory (DFT) showed that the bond dissociation energy of the O−H bond of the 4′-phenol is constant along the homologue series in contrast to $\Delta\mu$, the change in dipole moment upon hydrogen atom donation, which increases for increasing chain length. The frontier orbital energy gap goes through a maximum for D12. The change in the A-to-B dihedral angle upon hydrogen atom donation further shows a maximum for D12 of 6.45°. The importance of these microscopic properties for antioxidative activity was confirmed by a change in liposome fluorescence anisotropy using a fluorescent probe showing maximal penetration into the lipid bilayer for D12 along the homologue series.

KEYWORDS: isoflavonoid, daidzein derivative, antioxidation, dipole moment, frontier orbital energy gap

INTRODUCTION

Flavonoids and isoflavonoids show a rich structural diversity, which affects their bioactivity including their influence on cellular redox status as potential antioxidants and prooxidants.[1−4] The antioxidative effect of isoflavonoids and their glycosides, usually as important constituents present in many Asian foods, has been demonstrated in biological systems and in model systems.[5,6] As one representative of those most studied, the isoflavonoids, daidzein has been shown to be a prooxidant in liposomes and to completely lack cellular antioxidant activity,[1,2] but it has also been considered as an efficient radical scavenger and its *C*-glycoside puerarin an efficient antioxidant.[5,7]

The balance between antioxidative and prooxidative properties depends on the oxidation substrates, structural organization, and the microenvironment for the bioactive compound in addition to external factors such as heat, pressure, and exposure to light.[6,8,9] From the earlier review of Porter[10] to the most recent studies,[11,12] it has been realized that interfacial phenomena including more complex factors than polarity and lipid/water partition of bioactive compounds need to be taken into consideration for an understanding of the oxidative stability of heterogeneous lipid/water systems such as emulsions and liposomes. On the basis of lipophilization of phenolic antioxidants such as rosmarinic acid and chlorogenic acid through formation of alkyl esters and evaluation of their antioxidative efficacy, nonlinear effects of alkyl chain length have been described in terms of the so-called cutoff theory.[11,13] The rationale behind this theory seems, however, not clear, and different experimental strategies have been suggested to provide a better understanding.[11−13]

Daidzein, with only two phenolic groups and under certain conditions known as a prooxidant, was selected as the parent molecule for the synthesis of a series of 7-*n*-alkoxy daidzein derivatives to be tested as antioxidants. Theoretical calculations of relevant molecular properties of members of this homologue series were further hoped to provide help to explain the balance between prooxidative and antioxidative properties.

MATERIALS AND METHODS

Chemicals. Daidzein (>98%) was purchased from Huike Plant Exploitation, Inc. (Shanxi, China). 8-Anilino-1-naphthalenesulfonic acid (ANS), soybean L-*R*-phosphatidylcholine (PC), 2,2′-azinobis(3-ethylbenzothiazoline-6-sulfonic) acid (ABTS), and 2,2′-azobis(2-methylpropionamidine) dihydrochloride (AAPH) were from Sigma-Aldrich Chemical Co. (St. Louis, MO). 1-Bromoalkanes (1-bromo-*n*-butane), 1-bromo-*n*-octane, and 1-bromo-*n*-hexadecane, >98%), potassium persulfate (>99%), methanol (analytical grade), ethanol (HPLC grade), and chloroform (>99%) were purchased from Beijing Chemical Plant (Beijing, China). 1-Bromo-*n*-dodecane was from J&KChemica (Beijing, China), and 16-(9-anthroyloxy)palmitic acid (16-AP) was synthesized from 16-hydroxyhexadecanoic acid and 9-anthracenecarboxylic acid.[14]

Synthesis of 7-*n*-Alkoxy Derivatives (D4, D8, D12, and D16). Daidzein (1.0 g, 0.0039 mol) was dissolved in 20 mL of DMF and stirred at room temperature vigorously until it was completely dissolved.

Received: July 29, 2011
Revised: October 18, 2011
Accepted: October 18, 2011
Published: October 18, 2011

NaOH (~1.2 mol equiv, 0.0047 mol) and 0.08 g of KI were added into the working mixture. The addition of 0.0078 mol of 1-bromoalkane (1-bromo-*n*-butane, 1-bromo-*n*-octane, 1-bromo-*n*-dodecane, or 1-bromo-*n*-hexadecane) followed, and the temperature was kept at 120 °C for 1.5 h. The mixture was poured into 50 mL of stirred water, and then the pH was adjusted to 5−7. After filtration, the pellet was washed with water three times and then dried. Finally, the pellet was purified by silica gel chromatography eluted with a mixture of ethyl acetate/dichloromethane (1:5, v/v); each of the derivatives was collected with R_f values of ~0.3−0.4 and appeared as colorless crystalline plates. The yields were 62, 57, 56, and 45% for D4, D8, D12, and D16, respectively. All of the derivatives were characterized by nuclear magnetic resonance (NMR) and mass spectroscopies.

D4: ^{1}H NMR (400 M, d^6-DMSO), δ 0.95 (t, 3H, J = 7.2 Hz, $-CH_3$), 1.47 (m, 2H, $-CH_2-$), 1.75 (m, 2H, $-CH_2-$), 4.12 (t, 2H, J = 6.4 Hz, $-OCH_2-$), 6.83 (dd, 2H, J = 8.8 Hz, 3′-H, 5′-H), 7.05 (dd,1H, J = 8.8, 2.4 Hz, 6-H), 7.13 (d, 1H, J = 2.4 Hz, 8-H), 7.40 (dd, 2H, J = 8.4 Hz, 2′-H, 6′-H), 8.02 (d, 1H, J = 8.8 Hz, 5-H), 8.36 (s, 1H, 2-H), 9.55 (s, 1H, 4′−OH); ^{13}C NMR (400 M, d^6-DMSO), δ 14.2 ($-CH_3$), 19.2 ($-CH_2$), 31.0 ($-CH_2$), 68.7 ($-OCH_2$), 101.4 (8-C), 115.4 (6-C, 3′-C, 5′-C), 118.0 (10-C), 122.9 (1′-C), 124.2 (3-C), 127.4 (5-C), 130.5 (2′-C, 6′-C), 153.6 (2-C), 157.7 (9-C), 157.9 (4′-C), 163.5 (7-C), 175.2 (4-C); MS, m/z 311.12 $(M + H)^+$.

D8: ^{1}H NMR (400 M, d^6-DMSO), δ 0.86 (t, 3H, J = 6.4 Hz, $-CH_3$), 1.30 (m, 8H, $-(CH_2)_4-$), 1.43 (m, 2H, $-CH_2-$), 1.75 (m, 2H, $-CH_2-$), 4.11 (t, 2H, J = 6.4 Hz, $-OCH_2-$), 6.83 (dd, 2H, J = 8.8 Hz, 3′-H, 5′-H), 7.05 (dd,1H, J = 8.8, 2.4 Hz, 6-H), 7.12 (d, 1H, J = 2.4 Hz, 8-H), 7.41 (dd, 2H, J = 8.4 Hz, 2′-H, 6′-H), 8.02 (d, 1H, J = 8.8 Hz, 5-H), 8.36 (s, 1H, 2-H), 9.55 (s, 1H, 4′-OH); ^{13}C NMR (400 M, d^6-DMSO), δ 14.4 ($-CH_3$), 22.6, 25.9, 28.9, 29.1, 29.2, 31.7 ($-(CH_2)_6-$), 69.0 ($-OCH_2$), 101.4 (8-C), 115.4 (6-C, 3′-C, 5′-C), 118.0 (10-C), 122.9 (1′-C), 124.2 (3-C), 127.4 (5-C), 130.5 (2′-C, 6′-C), 153.6 (2-C), 157.7 (9-C), 157.9 (4′-C), 163.5 (7-C), 175.2 (4-C); MS, m/z 367.18 $(M + H)^+$.

D12: ^{1}H NMR (400 M, d^6-DMSO), δ 0.85 (t, 3H, J = 6.4 Hz, $-CH_3$), 1.24 (m, 16H, $-(CH_2)_8-$), 1.42 (m, 2H, $-CH_2-$), 1.75 (m, 2H, $-CH_2-$), 4.11 (t, 2H, J = 6.4 Hz, $-OCH_2-$), 6.83 (dd, 2H, J = 8.8 Hz, 3′-H, 5′-H), 7.05 (dd,1H, J = 8.8, 2.4 Hz, 6-H), 7.12 (d, 1H, J = 2.4 Hz, 8-H), 7.41 (dd, 2H, J = 8.4 Hz, 2′-H, 6′-H), 8.02 (d, 1H, J = 8.8 Hz, 5-H), 8.36 (s, 1H, 2-H), 9.55 (s, 1H, 4′-OH); ^{13}C NMR (400 M, d^6-DMSO), δ 14.4 ($-CH_3$), 22.6, 25.9, 28.9, 29.2, 29.2, 29.4, 29.4, 29.5, 29.5, 31.8 ($-(CH_2)_{10}-$), 68.9 ($-OCH_2$), 101.4 (8-C), 115.4 (6-C, 3′-C, 5′-C), 118.0 (10-C), 122.9 (1′-C), 124.2 (3-C), 127.4 (5-C), 130.5 (2′-C, 6′-C), 153.6 (2-C), 157.7 (9-C), 157.9 (4′-C), 163.5 (7-C), 175.2 (4-C); MS, m/z 423.25 $(M + H)^+$.

D16: ^{1}H NMR (400 M, d^6-DMSO), δ 0.85 (t, 3H, J = 6.4 Hz, $-CH_3$), 1.23 (m, 24H, $-(CH_2)_{12}-$), 1.43 (m, 2H, $-CH_2-$), 1.76 (m, 2H, $-CH_2-$), 4.12 (t, 2H, J = 6.4 Hz, $-OCH_2-$), 6.82 (dd, 2H, J = 8.8 Hz, 3′-H, 5′-H), 7.05 (dd, 1H, J = 8.8, 2.4 Hz, 6-H), 7.13 (d, 1H, J = 2.4 Hz, 8-H), 7.41 (dd, 2H, J = 8.4 Hz, 2′-H, 6′-H), 8.02 (d, 1H, J = 8.8 Hz, 5-H), 8.37 (s, 1H, 2-H), 9.54 (s, 1H, 4′-OH); ^{13}C NMR (400 M, $CDCl_3$), δ 14.1 ($-CH_3$), 22.7, 26.0, 29.0, 29.4, 29.4, 29.5, 29.5, 29.6, 29.6, 29.7, 29.7, 29.7, 29.7, 31.9 ($-(CH_2)_{14}-$), 68.8 ($-OCH_2$), 100.6 (8-C), 115.0 (6-C), 115.7 (6-C, 3′-C, 5′-C), 118.2 (10-C), 124.0 (1′-C), 125.1 (3-C), 127.8 (5-C), 130.4 (2′-C, 6′-C), 152.2 (2-C), 156.0 (9-C), 158.1 (4′-C), 163.7 (7-C), 176.3 (4-C); MS, m/z 479.31 $(M + H)^+$.

Molar Extinction Coefficient (ε) Measurements. The molar extinction coefficients (ε) of daidzein (D) and its 7-*n*-alkoxy derivatives (D4, D8, D12, D16) were measured in methanol on a Cary50 spectrophotometer (Varian Inc., Palo Alto, CA) with a standard quartz cuvette (optical path length = 1 cm), and ε was determined on the basis of the Lambert−Beer law by linear regression fitting to the data of absorbance versus absolute sample concentration.

Cyclic Voltammetric Measurements. Cyclic voltammetry was performed on a CHI660B potentiostat (Chenghua, Shanghai, China) with a three-electrode configuration,[15] for which daidzein (D) and its 7-*n*-alkoxy derivative (D4, D8, D12, D16) solutions at a concentration of 5.4×10^{-4} M in dry tetrahydrofuran were used. The tetrahydrofuran was dried by refluxing over sodium metal for 24 h under nitrogen protection, which was then distilled into a flask under nitrogen atmosphere by using the vapor transfer method. The final concentration of supporting electrolyte, polarographic grade tetra-*n*-butylammonium hexafluorophosphate (TBHFP), was made at 0.1 M. The working electrode was a glassy carbon piece (diameter = 4 mm); the reference electrode was a silver wire pseudoreference electrode calibrated against the ferrocene/ferrocenium couple; and the counter electrode was a platinum wire. To expel oxygen, all of the solution preparation and the electrochemical cell setup were performed in a nitrogen-charged glovebox. All of the measurements were done at 25 °C. The oxidative peak potential was obtained by subtracting the practical potential of the Ag/AgCl electrode, 0.104 V, calculated on the concentration of Ag^+ of 0.01 M in THF.

Trolox Equivalent Antioxidant Capacity (TEAC). The radical scavenging assay was based on the stoichiometry of the reaction of (iso)flavones with $ABTS^{\bullet+}$.[16] Potassium persulfate was added to a solution of 7 mM ABTS (final concentration = 2.45 mM), which was kept at a constant temperature for 12 h in the dark to generate $ABTS^{\bullet+}$.[17] The final concentrations of scavengers and $ABTS^{\bullet+}$ were 1.0×10^{-5} and $(1.0-5.5) \times 10^{-5}$ M, respectively. The reaction kinetics of scavenging $ABTS^{\bullet+}$ were followed by monitoring its characteristic absorption at 734 nm ($\varepsilon_{734\ nm} = 1.5 \times 10^4$ L mol^{-1} cm^{-1}) at 25 °C. The absorbance difference before and after reaction ($\Delta A_{734\ nm}$) was plotted against the ABTS concentration and was fitted to the relationship $\Delta A_{734\ nm} = a(1 - e^{-bc})$. The TEAC values of daidzein and 7-*n*-alkoxy derivatives were then obtained as TEAC = $a/(\varepsilon_{734\ nm} C_{sample} \times 1.9)$, where 1.9 was the antioxidant capacity of Trolox.

Evaluation of Antioxidation in Liposome. Liposome was prepared by using an extrusion method. Briefly, PC (6.75 mg) was dissolved in absolute chloroform (10 mL), and then the daidzein and its 7-*n*-alkoxy derivatives dissolved in 5 mL of absolute methanol (15 μM) were added to a 100 mL flask. The solvent was then removed by rotary evaporation at ~20 °C. Nitrogen gas was introduced to re-establish atmospheric pressure, and the flask was covered with aluminum foil. Then, an oil-free vacuum pump was used to maintain the flask vacuum at <0.5 mmHg for >1 h. The lipid residue was rehydrated with phosphate buffer (45 mL, 10 mM, pH 7.40). The flask was then shaken while being sonicated for 1 min, producing a homogeneous white suspension of multilamellar liposomes. Then 5 mL of the water-soluble radical initiator AAPH (2.5 mM) in sodium phosphate buffer (pH 7.40) was added for the initiation of lipid peroxidation from the aqueous phase. Unilamellar liposomes were obtained by pushing the multilamellar liposome solution through the polycarbonate membrane with 100 nm sieve pores (Whatman, Maidstone, U.K.) 20 times. The final concentrations of the antioxidants and AAPH in the liposome suspension were 1.5 and 250 μM, respectively.

Evaluation of Membrane Fluidity. The effects of antioxidants on membrane fluidity were evaluated using the fluorescent probes 16-AP[18] and ANS.[19] Daidzein and its 7-*n*-alkoxy derivatives (4.5 μM) were added to the liposome suspension (150 μM) and were added with ANS in the stock phosphate buffer solution (10 mM, pH 7.4) to yield a final concentration of 25 μM. The preparation were incubated at 43 °C for 5 min. Fluorescence spectra (420−600 nm) were measured on an LS-55 luminescence spectrophotometer (Perkin-Elmer, Beaconsfield, U.K.) under excitation at 400 nm. To evaluate the influence of antioxidants on the fluidity of the interior of lipid bilayer, 16-AP was added to the PC solution during the preparation of the liposome (final concentration = 0.5 μM), and the preparation were then obtained by adding a 4.5 μM sample and incubating at 43 °C for 5 min. Fluorescence polarization (P) was determined at 415 nm (excited at 380 nm)

according to the relationship $P = (I_{||} - GI_{\perp})/(I_{||} + GI_{\perp})$, where $I_{||}$ and $I_{\perp}$ represent the fluorescence intensities measured with the emission polarization parallel and vertical to the excitation polarization, respectively, and G stands for the instrumental polarization factor, which was determined to be ~1.

Quantum Mechanical Calculations. The molecular geometries of the five compounds and their deprotonated and oxidized forms were optimized with the UB3LYP density functional theory (DFT) in conjunction with the 6-31G(d,p) basis set by the use of the Gaussian 03 package.[20] The gas-phase deprotonation enthalpy (DE) and bond dissociation energy (BDE) were derived as the enthalpy differences of the reactions ArOH → ArO^- + H^+ and ArOH → $ArO^{\bullet}$ + $H^{\bullet}$, respectively.

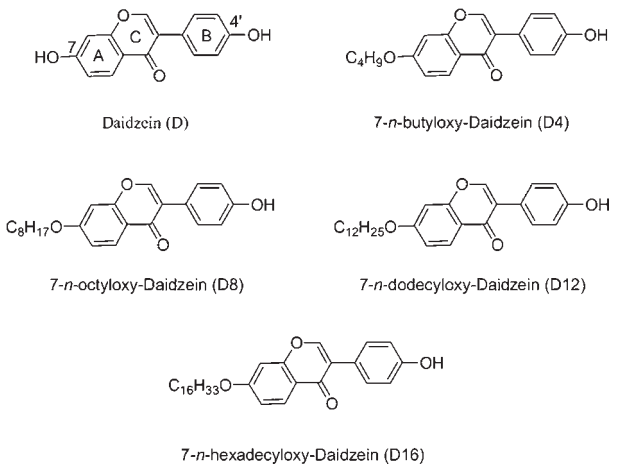

Figure 1. Structures of daidzein and its 7-*n*-alkoxy derivatives.

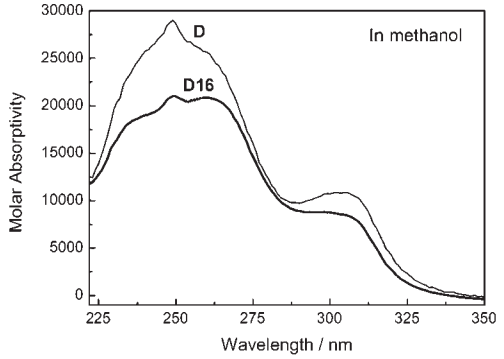

Figure 2. Absorption spectra of daidzein (D) and 7-*n*-hexadecyloxy-daidzein (D16). The spectra of D4, D8, and D12 are similar to that of D16.

RESULTS AND DISCUSSION

Four homologue 7-*n*-alkoxydaidzeins (Figure 1) were obtained by Williamson synthesis, purified, and characterized by ^{1}H NMR and MS. The UV−visible spectrum is only marginally affected by the ether formation (cf. Figure 2 and Table 1). The presence of the hydrophobic alkyl chain makes the series increasingly water insoluble, in effect preventing a determination of the *n*-octanol/water partition coefficient. The calculated

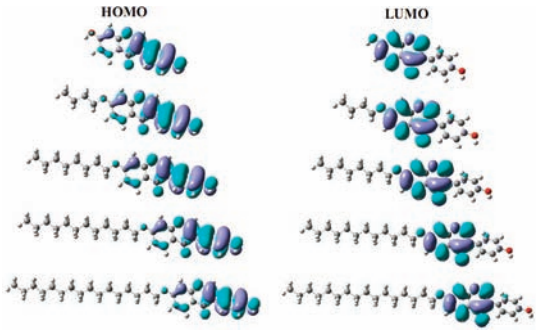

Figure 3. DFT-optimized geometry and charge density of molecular orbital of highest occupied molecular orbital (HOMO) and lowest unoccupied molecular orbital (LUMO) for daidzein and its 7-*n*-alkoxy derivatives in the gas phase using the B3LYP method and 6-31G (d, p) basis set.

Table 1. Absorption Maximum (λ_{max}), Molar Absorptivity (ε_{max}), Calculated *n*-Octanol/Water Partition Coefficient (Clog*D*), Calculated Dipole Moment (μ) for Parent Compound and Phenoxyl Radical, Calculated A-to-B Dihedral Angle (α) for Phenol and Phenoxyl Radical, Calculated Deprotonation Energy (DE), Bond Dissociation Energy (BDE), and Energy of the Frontier Orbital E_{HOMO}/E_{LUMO} and Their Difference (ΔE) for Daidzein and Its 7-*n*-Alkoxy Derivatives

	daidzein (D)	7-*n*-butyloxy-D	7-*n*-octyloxy-D	7-*n*-dodecyloxy-D	7-*n*-hexadecyloxy-D
λ_{max}/nm [a]	249, 305	249, 260, 307	249, 260, 307	249, 260, 307	249, 260, 307
$\varepsilon_{249\ nm}$/L mol^{-1} cm^{-1} [a]	2.9×10^4	2.0×10^4	2.3×10^4	2.1×10^4	2.1×10^4
Clog$D_{7.4}$ [b]	1.55	4.04	5.91	7.99	9.66
μ(phenol)	2.21	3.36	3.50	3.54	3.55
μ(phenoxyl)	7.75	9.14	9.32	9.38	9.40
$\Delta\mu$ [c]	5.54	5.78	5.82	5.84	5.85
α/degree (phenol)	36.44	36.43	36.31	36.61	36.50
α/degree (phenoxyl)	30.72	30.50	30.30	30.26	30.37
$\Delta\alpha$ [d]	5.72	5.93	6.01	6.45	6.13
DE/kJ mol^{-1}	1500	1503	1503	1503	1503
BDE/kJ mol^{-1}	368.1	367.2	367.1	367.1	367.1
E_{HOMO}/eV	−5.6265	−5.5623	−5.5576	−5.5582	−5.5574
E_{LUMO}/eV	−1.3812	−1.3153	−1.3096	−1.3083	−1.3080
ΔE/eV [e]	4.2453	4.2470	4.2480	4.2499	4.2494

[a] In methanol and at 25 °C. [b] pH 7.4 for aqueous phase. [c] $\Delta\mu = \mu$(phenoxyl) − μ(phenol). [d] $\Delta\alpha = \alpha$(phenoxyl) − α(phenol). [e] $\Delta E = E_{LUMO} - E_{HOMO}$.

Table 2. Oxidation Potentials (V) in Tetrahydrofuran, Trolox Equivalent Antioxidant Capacity (TEAC) for Radical Scavenging, and Lag Phase Index (LPI) for Liposome Peroxidation Initiated in the Lipid Phase for Daidzein (D) and Its 7-*n*-Alkoxy Derivatives

	daidzein (D)	7-*n*-butyloxy-D	7-*n*-octyloxy-D	7-*n*-dodecyloxy-D	7-*n*-hexadecyloxy-D
E (vs NHE)[a]	1.09	1.08	1.05	0.98	0.94
TEAC[a]	1.96	0.67	0.52	0.41	0.33
LPI[b]	0.89 ± 0.03	0.77 ± 0.02	1.16 ± 0.06	1.39 ± 0.06	1.20 ± 0.03

[a] Measured at 25 °C. [b] Measusred at 43 °C (mean of three determinations with the lag phase for blank (LPI = 1.00) ranging between 30.6 and 32.8 min, see Figure 5).

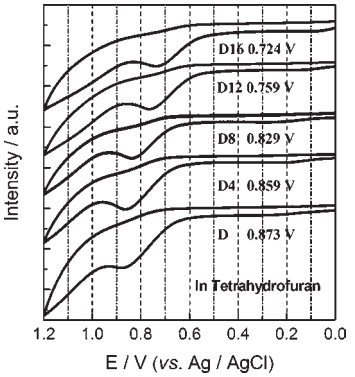

Figure 4. Cyclic voltammograms of 5.0×10^{-4} M daidzein (D) and its 7-*n*-alkoxy derivatives (D4, D8, D12, and D16) in neutral tetrahydrofuran at 25 °C. Oxidative peak potentials indicated are versus Ag/AgCl.

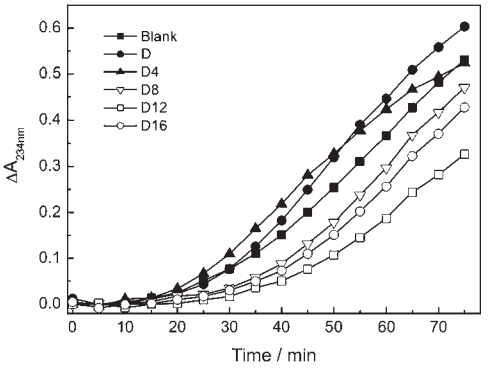

Figure 5. Oxidation of phosphatidylcholine in liposomes at 43 °C as monitored spectrophotometrically at 234 nm through formation of conjugated dienes following initiation by hydrophilic free radical initiator AAPH (250 μM). The lag phase for oxidation was determined in the absence (blank) and presence of daidzein (D) and its 7-*n*-alkoxy derivatives, D4, D8, D12, and D16, each at a concentration of 4.5 μM.

values for the condition of pH 7.4, C$\log D_{7.4}$, confirm the expected increased lipophilicity (cf. Table 1).

Quantum mechanical calculations within the DFT provided the optimized geometries for the five compounds in the gas phase, which all showed a linear conformation of the alkyl chain and noncoplanarity of the A and B rings. The 4′-phenol is the most reducing of the two phenolic groups in daidzein, and the charge density of the highest occupied molecular orbital (HOMO) confirmed the B-ring phenol as reactive for electron transfer (reduction). The lowest unoccupied molecular orbital (LUMO) has, in contrast, highest density in the A and C rings for all five compounds (cf. Figure 3). The dipole moment, μ, of the five compounds increases asymptotically from 2.21 D for daidzein (D) to 3.55 D for D16 (Table 1). The A-to-B dihedral angle, α, shows, in contrast, a slight decrease from D to D8 followed by an increase for D12, as seen from Table 2. Upon one-electron oxidation followed by deprotonation or upon hydrogen atom transfer as expected for radical scavenging by the compounds

$$R{-}OH \rightarrow R{-}O^{\bullet} + H^{\bullet} \quad (1)$$

a 4′-phenoxyl radical is formed. From the DFT calculations, μ and α became available also for the homologue radical series as included in Table 1. Notably, the change in dipole moment, $\Delta\mu$, upon radical formation changes asymptotically from 5.54 D for D to 5.85 D for D16, whereas $\Delta\alpha$ shows a significant maximum for D12. The bond dissociation energy (BDE), corresponding to the reaction of eq 1, changes only from D to D4 and remains constant for the longer alkyl substituents, and a similar pattern is seen for dissociation energy (DE) related to the pK_a values corresponding to the reaction

$$R{-}OH \rightarrow R{-}O^{-} + H^{+} \quad (2)$$

The energy of the frontier orbitals shows for HOMO a maximum for D12, whereas for LUMO, a slightly gradual decrease is seen along the series. The energy gap between the frontier orbitals, ΔE, shows, as a result of these different trends for HOMO and LUMO, a maximum value for D12 like $\Delta\alpha$. The oxidation potential for the homologues as determined by cyclic voltammetry is related to the BDE as a microscopic property determined for the gas phase. *E* changes, however, in contrast to BDE, along the series, making the compounds increasingly reducing for increasing alkyl length (cf. Figure 4 and Table 1). The values of *E* were determined in tetrahydrofuran, a moderately polar solvent, which seems to stabilize the radicals, R−O$^{\bullet}$, compared to the phenols, R−OH, of eq 1, for increasing $\Delta\mu$. The largest decrease in *E* between two homologues is seen when D8 and D12 are compared. Notably, for $\Delta\alpha$, the change in the A-to-B dihedral angle upon hydrogen atom abstraction, the largest change is likewise seen between D8 and D12.

The antioxidant capacity was determined for the homologue series, and for the parent compound D, a value close to 2 was found for TEAC, as expected for a diphenol.[2] For the alkyl derivatives, which notably have only a single phenolic group, the TEAC value decreased gradually from D8 to D16 (see Table 2). The decrease may be due to solvent effects because the TEAC method involves water as solvent, in which the higher homologues may aggregate, showing less reactivity. The efficacy of the compounds D−D16 as antioxidants was tested in a liposome system with initiation in the aqueous phase. The incorporation of the compounds was monitored by fluorescence spectroscopy using a fluorescence probe (ANS) for bilayer surface rigidity together with a probe (16-AP) for membrane fluidity.[6] The addition of D−D16 to the liposomes enhanced the fluorescence, showing that each of the compounds was incorporated in the surface (Figure 6A). The fluorescence enhancement is induced

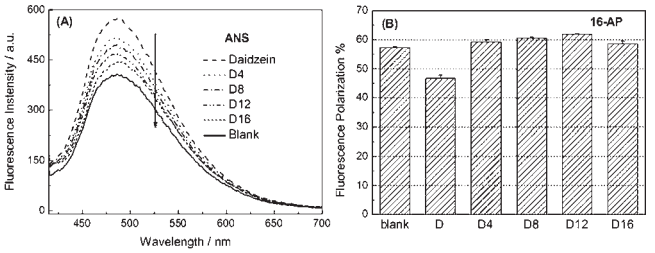

Figure 6. (A) Fluorescence spectra of liposome suspension containing 8-anilino-1-naphthalenesulfonic acid (ANS) fluorophore (25 μM) and daidzein or its 7-*n*-alkoxy derivative D4, D8, D12, and D16. (B) Fluorescence polarization of 16-(9-anthroyloxy)palmitic acid (16-AP, 0.5 μM) as a function of addition of daidzein (D) or its 7-*n*-alkoxy derivatives D4, D8, D12, and D16 following incubation at 43 °C .

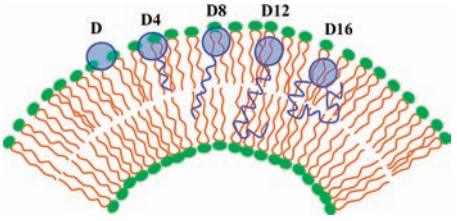

Figure 7. Schematic model of daidzein and its 7-*n*-alkoxy derivative deposition into liposome lipid/water interface.

by an increase in ANS molecules incorporated in the membrane. The concentration of D and derivatives in the proximity of the membrane surface follows the order D > D4 > D8 > D12 > D16, in agreement with the lipophilicity as quantified by Clog$D_{7.4}$. The fluorescence polarization of 16-AP is known to increase with a decrease in membrane fluidity. From the results presented in Figure 6B, it is seen that the membrane fluidity increases by the addition of D, whereas for D4−D16 the fluidity decreases, indicating the presence of the compounds in the central domain of the bilayer according to the order D12 > D8 > D4 > D16 > D.

The presence of the compounds in the surface proximity and in the central domain of the bilayer is expected to follow the reverse order as confirmed by the experiments except for D16, which is present to a lesser degree in the central domain of the bilayer than expected. The alkyl chain of D16 is suggested to coil, deviating from the linearity found for the gas phase (Figure 3). D16 is accordingly suggested to concentrate in an intermediate region as shown in Figure 7.

The balance between prooxidative and antioxidative effects of daidzein and the homologue series of alkyl derivatives was investigated by monitoring the appearance of primary lipid oxidation products in liposomes with lipid oxidation initiated in the aqueous phase in the presence and absence of the compounds D−D16. The result of one such experiment is seen in Figure 5. D and D4 are seen to be prooxidants, whereas D8, D12, and D16 are antioxidants for the actual experimental conditions. Notably, D12 is more efficient as an antioxidant than both D8 and D16. A lag phase index (LPI) for lipid oxidation in the liposomes, LPI = lag phase (antioxidant)/lag phase (blank), is collected in Table 2 on the basis of three independent experiments. Notably, LPI < 1 indicates prooxidative effects, whereas LPI > 1 indicates antioxidative effects.

On the basis of an analysis of the antioxidative activity of 27 flavonoids using the method of quantitative structure−activity

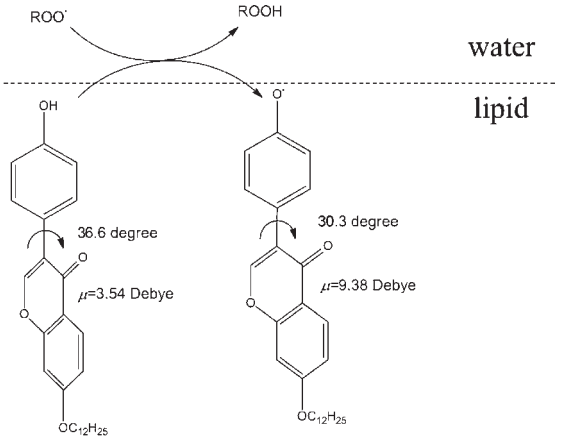

Figure 8. 7-*n*-Dodecyloxydaidzein reacting in the lipid/water interface with a peroxyl radical generated in the liposome aqueous phase.

relationship (QSAR) using molecular descriptors obtained by DFT calculations, topological descriptors, and indicator descriptors, it was concluded that the dipole moment rather than frontier orbital energies or bond dissociation energies were important for antioxidative activity as measured as inhibition of lipid peroxidation in homogenates of liver and blood of rats.[21] In the present study, the value of BDE, which showed little variation, was not found directly correlated with the antioxidative effect in the liposome system. This may seem unexpected provided the general importance of the strength of the O−H bond for the magnitude of the standard reduction potentials and for radical scavenging.[22] However, this result is in agreement with the results of the QSAR study of flavonoids.[21]

Among the microscopic properties for the D−D16 series of compounds obtained by quantum mechanical calculations, the dipole moment shows a variation that would predict that the antioxidative efficacy would approach a limit for increasing the alkyl length to eight carbons and above. This is clearly not seen, and neither μ nor $\Delta\mu$ during formation of phenoxyl radicals gives any indication of the nonlinear behavior observed with the decrease in efficacy for D16. The energy gap for the frontier molecular orbitals provides, however, an indication of a discontinuity, as ΔE has a maximal value for D12, the most efficient of the derivatives tested as antioxidant. Similarly, $\Delta\alpha$, the change in the A-to-B dihedral angle, shows a clear maximum along the series for D12. The flexibility of rotation for the B ring relative to the A ring of (iso)flavonoids has previously been found to be important for high antioxidant efficiency at lipid/water interfaces.[2] Equol is thus an efficient antioxidant despite the lack of conjugation between the B and AC rings but with a high structural flexibility.[2] Catechins, which are known to be very efficient as antioxidants in heterogeneous systems, likely have a facile rotation of the B ring relative to the AC ring system.[23]

The microscopic properties of the D−D16 series of prooxidants/antioxidants at lipid/water interfaces seem accordingly to give indications of a discontinuity, leaving the D12 as the most effective antioxidant. A deeper understanding based on the molecular structure will have to await DFT calculations for which solvent effects and effects of the lipid bilayer are included. Such strenuous calculations are expected to confirm deviations from the linearity of the alkyl chain of the daidzein derivatives. However, the microscopic parameters now shown to have maximal values for D12 are clearly in the manifestation of optimal

antioxidant efficacy for D12. Fluorescence spectroscopy further has shown that the location among the homologues becomes optimal for D12, which may relate both to the flexibility of the B ring and to a coiling of the alkyl chain for homologues higher than D12 as illustrated in Figure 7. The balance between surface protection of the liposomes against radical generated in the aqueous phase and modulation of membrane fluidity accordingly seems to be important and to relate to the B-ring flexibility and the frontier orbital energy gap of the radical scavenger.[18,24] In Figure 8 the critical process for the antioxidant activity of D12 is illustrated with the important microscopic properties indicated.

AUTHOR INFORMATION

Corresponding Author

*(P.W.) E-mail: wpeng@iccas.ac.cn. Phone: +86-10-62516604. Fax: +86-10-62516444. (L.H.S.) E-mail: ls@life.ku.dk. Phone: +45 3528 3221. Fax: +45 3528 3344.

Funding Sources

This work has been supported by the Natural Science Foundation of China (20803091), the Fundamental Research Funds for the Central Universities, and the Research Funds of Renmin University of China (RUC 10XNI007 and RUC 11XNI003). L.H.S. is grateful for support from the Danish Research Council for Technology and Production through Grant 09-065906/FTP: Redox communication in the digestive tract.

REFERENCES

(1) Wolfe, K. L.; Liu, R. H. Structure activity relationships of flavonoids in the cellular antioxidant activity assay. *J. Agric. Food Chem.* **2008**, *56*, 8404–8411.

(2) Han, R.-M.; Tian, Y.-X.; Liu, Y.; Chen, C.-H.; Ai, X.-C.; Zhang, J.-P.; Skibsted, L. H. Comparison of flavonoids and isoflavonoids as antioxidants. *J. Agric. Food Chem.* **2009**, *57*, 3780–3785.

(3) Qiong, G.; Rimbach, G.; Moini, H.; Weber, S.; Packer, L. ESR and cell culture studies on free radical-scavenging and antioxidant activities of isoflavonoids. *Toxicology* **2002**, *179*, 171–178.

(4) Wiiliams, R. J.; Spencer, J. P. E.; Rice-Evans, C. A. Flavonoids: antioxidants or signalling molecues. *Free Radical Biol. Med.* **2004**, *36*, 838–849.

(5) Jiang, B.; Liu, J. H.; Bao, Y. M.; An, L. J. Hydrogen peroxide-induced apoptosis in pcl2 cells and the protective effect of puerarin. *Cell Biol. Int.* **2003**, *27*, 1025–1031.

(6) Liang, J.; Tian, Y.-X.; Fu, L.-M.; Wang, T.-H.; Li, H.-J.; Wang, P.; Han, R.-M.; Zhang, J.-P.; Skibsted, L. H. Daidzein as an antioxidant of lipids: effects of the microenvironment in relation to chemical structure. *J. Agric. Food Chem.* **2008**, *56*, 10376–10383.

(7) Han, R.-M.; Chen, C.-H.; Tian, Y.-X.; Zhang, J.-P.; Skibsted, L. H. Fast regeneration of carotenoids from radical cations by isoflavonoid dianions: importance of the carotenoid keto group for electron transfer. *J. Phys. Chem. B* **2010**, *114*, 126–132.

(8) Shahidi, F.; Zhong, Y. Lipid oxidation and improving the oxidative stability. *Chem. Soc. Rev.* **2010**, *39*, 4067–4079.

(9) Frankel, E.; Huang, S. W.; Ranner, J.; German, J. B. Interfacial phenomena in the evaluation of antioxidants: Bulk oils vs emulsions. *J. Agric. Food Chem.* **1994**, *42*, 1054–1059.

(10) Porter, W. L. Paradoxical behavior of antioxidants in food and biological systems. In *Antioxidants: Chemical, Physiological, Nutritional and Toxicological Aspects*; Williams, G. M., Ed.; Princeton Scientific: Princeton, NJ, 1993; pp 93−122.

(11) Laguerre, M.; Giraldo, L. J. L.; Lecomte, J.; Figueroa-Espinoza, M.-C.; Baréa, B.; Weiss, J.; Decker, E. A.; Villeneuve, P. Chain length affects antioxidant properties of chlorogenate esters in emulsion: the cutoff theory behind the polar paradox. *J. Agric. Food Chem.* **2009**, *57*, 11335–11342.

(12) Shahidi, F.; Zhong, Y. Revisiting the polar paradox theory: a critical overview. *J. Agric. Food Chem.* **2011**, *59*, 3499–3504.

(13) Laguerre, M.; Giraldo, L. J. L.; Lecomete, J.; Figueroa-Espinoza, M.-C.; Baréa, B.; Weiss, J.; Decker, E. A.; Villeneuve, P. Relationship between hydrophobicity and antioxidant activity of "phenolipids" in emulsion: a parabolic effect of chain length of rosmarinate esters. *J. Agric. Food Chem.* **2010**, *58*, 2869–2876.

(14) Tilley, L.; Thulborn, K. R.; Sawyer, W. H. An assessment of the fluidity gradient of the lipid bilayer as determined by a set of *n*-(9-anthroyloxy) fatty acids (*n*) 2, 6, 9, 12, 16). *J. Biol. Chem.* **1979**, *8*, 2592–2594.

(15) Luo, H. X.; Shi, Z. J.; Li, N. Q.; Gu, Z. N.; Zhuang, Q. K. Investigation of the electrochemical and electrocatalytic behavior of single-wall carbon nanotube film on a glassy carbon electrode. *Anal. Chem.* **2001**, *73*, 915–920.

(16) Sekher Pannala, A.; Chan, S. T.; O'Brien, P. J.; Rice-Evans, C. A. Flavonoid B-ring chemistry and antioxidant activity: Fast reaction kinetics. *Biochem. Biophys. Res. Commun.* **2001**, *282*, 1161–1168.

(17) Re, R.; Pellegrini, N.; Proteggente, A.; Pannala, A.; Yang, M.; Rice-Evans, C. A. Antioxidant activity applying an improved ABTS radical cation decolorization assay. *Free Radical Biol. Med.* **1999**, *26*, 1231–1237.

(18) Arora, A.; Byrem, T. M.; Nair, M. G.; Strasburg, G. M. Modulation of liposomal membrane fluidity by flavonoids and isoflavones. *Arch. Biochem. Biophys.* **2000**, *373*, 102–109.

(19) Jagannadham, M. V.; Rao, V. J.; Shivaji, S. The major carotenoid pigment of a psychrotrophic *Micrococcus roseus* strain: purification, structure, and interaction with synthetic membranes. *J. Bacteriol.* **1991**, *173*, 7911–7917.

(20) Frisch, M. J.; Trucks, G. W.; Schlegel, H. B.; Scuseria, G. E.; Robb, M. A.; Cheeseman, J. R.; Montgomery, J. A., Jr.; Vreven, T.; Kudin, K. N.; Burant, J. C.; Millam, J. M.; Iyengar, S. S.; Tomasi, J.; Barone, V.; Mennucci, B.; Cossi, M.; Scalmani, G.; Rega, N.; Petersson, G. A.; Nakatsuji, H.; Hada, M.; Ehara, M.; Toyota, K.; Fukuda, R.; Hasegawa, J.; Ishida, M.; Nakajima, T.; Honda, Y.; Kitao, O.; Nakai, H.; Klene, M.; Li, X.; Knox, J. E.; Hratchian, H. P.; Cross, J. B.; Bakken, V.; Adamo, C.; Jaramillo, J.; Gomperts, R.; Stratmann, R. E.; Yazyev, O.; Austin, A. J.; Cammi, R.; Pomelli, C.; Ochterski, J. W.; Ayala, P. Y.; Morokuma, K.; Voth, G. A.; Salvador, P.; Dannenberg, J. J.; Zakrzewski, V. G.; Dapprich, S.; Daniels, A. D.; Strain, M. C.; Farkas, O.; Malick, D. K.; Rabuck, A. D.; Raghavachari, K.; Foresman, J. B.; Ortiz, J. V.; Cui, Q.; Baboul, A. G.; Clifford, S.; Cioslowski, J.; Stefanov, B. B.; Liu, G.; Liashenko, A.; Piskorz, P.; Komaromi, I.; Martin, R. L.; Fox, D. J.; Keith, T.; Al-Laham, M. A.; Peng, C. Y.; Nanayakkara, A.; Challacombe, M.; Gill, P. M. W.; Johnson, B.; Chen, W.; Wong, M. W.; Gonzalez, C.; Pople, J. A. *Gaussian 03*, revision C.02; Gaussian, Inc.: Wallingford, CT, 2004.

(21) Rasulev, B. F.; Abdullaev, N. D.; Syrov, V. N.; Leszczynski, J. A quantitative structure−activity relationship (QSAR) study of the antioxidant activity of flavonoids. *QSAR Comb. Sci.* **2005**, *24*, 1056–1065.

(22) Jørgensen, L. V.; Madsen, H. L.; Thomsen, M. K.; Dragsted, L. O.; Skibsted, L. H. Regeneration of phenolic antioxidants from phenoxyl radicals: an ESR and electrochemical study of antioxidant hierarchy. *Free Radical Res.* **1999**, *30*, 207–220.

(23) Rajiya, R.; Rumazawa, S.; Nakayama, T. Steric effects on interaction of tea catechins with lipid bilayers. *Biosci., Biotechnol., Biochem.* **2001**, *65*, 2638–2643.

(24) Oteiza, P. I.; Erlejman, A. G.; Verstraeteis, S. V.; Reen, C. L.; Fraga, C. G. Flavonoid−membrane interactions: a protective role of flavonoids of the membrane surface. *Clin. Dev. Immunol.* **2005**, *12*, 19–25.